3D Topology Preserving Flows for Viewpoint-Based Cortical Unfolding

Kelvin Rocha, Ganesh Sundaramoorthi, Anthony Yezzi
School of Electrical and Computer Engineering
Georgia Institute of Technology
Atlanta, GA USA
{krocha,ganeshs,ayezzi}@ece.gatech.edu

Abstract

We present a variational method for unfolding of the cortex based on a user-chosen point of view as an alternative to more traditional global flattening methods, which incur more distortion around the region of interest. Our approach involves two novel contributions. The first is an energy function and its corresponding gradient flow to measure the average visibility of a region of interest of a surface from a given viewpoint. The second is an additional energy function and flow designed to preserve the 3D topology of the evolving surface. This latter contribution receives significant focus in this paper as it is crucial to obtain the desired unfolding effect derived from the first energy functional and flow. Without it, the resulting topology changes render the unconstrained evolution uninteresting for the purpose of cortical visualization, exploration, and inspection.

1. Introduction

Active surfaces, the 3D version of active contours, comprise one of the primary tools for medical image segmentation. In most medical imaging applications, the topology of the object to be segmented is known in advance. As such, a number of researchers have endeavored to incorporate various topology preservation constraints into their evolution models for the purpose of segmentation. Some authors such as Han *et al*. [1, 2], in their work on cortical segmentation, have proposed discrete representation dependent constraints that kick in at the moment and at the location where a topology change is about to occur in order to enforce the original topology. Others, such as Unal *et al*. [3, 4] have directly added continuous evolution forces that increase toward infinity as the contour or surface configuration approaches a change in topology. Sundaramoorthi and Yezzi [5] recently introduced a variational method for

topology preservation in active contours based on knot energies [6, 7]. Other variational approaches for topology preservation are found in the work by Shi and Karl [8], which only favors the repulsion of different connected components of the evolving curves, and in the work of Alexandrov and Santosa [9] and the recent work of Le Guyader and Vese [10], both of which are designed specifically for Level Set Methods [11].

For many segmentation applications, the manner in which the topology constraints are introduced is often unimportant since only the final configuration of the contour matters. Here, however, we consider an application of cortical unfolding in which the evolution itself is important to the end user who will typically wish to stop the unfolding process at any given time to obtain the desired level of unfolding. Therefore, the nature of the topology preservation should go hand-in-hand with the desired unfolding evolution and not yield undesirable transient geometric configurations that are often common when using mere topology enforcement.

The extension of the global knot-energy based topology regularizers proposed in [5] to three dimensions is conceptually straight-forward but mathematically and computationally much more involved than the original 2D formulation. However, our effort seems to have been well justified since these types of topology preserving energies are ideally suited to our cortical unfolding application. The resulting evolution forces, on their own, induce an unfolding effect that tends to drive the initial cortical surface towards a final spherical configuration that globally minimizes most knot energies (see [7] for the case of curves). This renders a very natural and visually pleasing global unfolding effect.

Our goal is a viewpoint dependent unfolding of the cortex in which the user is able to select an area of interest on the cortical surface for visualization. By focusing the unfolding on a region of interest with respect to a chosen viewpoint, distortion effects may be significantly reduced compared with global flattening techniques [12, 13, 14] commonly used in brain mapping. To accomplish this, we introduce a novel energy functional and gradient flow to measure and improve the

average visibility of the selected region. Without topology preservation, however, this flow is not useful for the purpose of cortical visualization and unfolding. Since knot-energy based topology preservation forces already produce a more global unfolding effect on their own, they combine very naturally with our visibility based flows to maintain a constant topology without introducing undesirable artifacts into the evolution.

The remainder of this article is organized as follows. In Section 2 we review the two dimensional knot-energy based topology preservation method introduced in [5]. In Section 3 we outline the extension of this method to three dimensions. As the computations in the 3D case are significantly more involved compare with their 2D counterparts, we do not include all the intermediate calculations for reasons of space. In Section 4 we present our viewpoint based visibility energy functional and its corresponding gradient flow to which this 3D topology preservation method will be applied. It is important to note, however, that without the topology constraint, the visibility based flow often undergoes intermediate topology changes during the resulting cortical unfolding process. As such, while the visibility energy provides the driving force behind our flow, the topology forces are indispensable to this application. Finally, in Section 5 we show simulations on both synthetically created surfaces as well as cortical surfaces extracted from real data.

2. Background on Topology Preservation

In many active surfaces applications it is very important that the topology of the object does not change during the evolution. For instance, when the cortex of the brain is being segmented it is necessary to keep its topology during the evolution because the cortex is homeomorphic to a two dimensional sphere [1, 2].

A number of topology preservation methods have been proposed in the past. Hans et al. [1, 2] presented a technique to prevent topology changes when the active contour evolution is implemented via Level Sets Methods. In this work, changes in topology at grid points are detected by deriving a condition based on the configuration of the level set function in a small neighborhood of the grid points. This method has the disadvantage of being highly dependent on the grid spacing used in the level set function. In addition, when this method is used the resulting motion may be abrupt and look unnatural.

Unal *et al.* [3] proposed a novel approach for topology preservation for active polygons. In this work, it is assumed that the polygon consists of a uniform charge distributed along its perimeter. Each vertex is then moved in the direction of the electrostatic force, which is

computed numerically. Even though this method may prevent some topology changes, it does not prevent two adjacent sides from touching. Moreover, the flow is unstable as the number of vertices increases and the length of the segments decreases [3].

Sundaramoorthi and Yezzi [5] have proposed a robust topology preservation technique in which a special geometric flow is added to the original image based curve evolution to avoid intersections. This geometric flow, which is derived from the minimization of an energy based on electrostatic principles, affects significantly the original evolution only when the contour is close to a change in topology. Unlike a curvature regularizer, when the regularizer proposed in [5] is applied to a point the resulting force depends globally on all other points of the curve. This technique, which is based on the work in [6, 7], has the advantage over the one proposed in [1, 2] of changing the original evolution in a gradual manner. Moreover, it is not restricted to level sets and can be used on any active contour implementation.

Since the 3D topology preservation method we are proposing in this paper is an extension of the work in [5], in the rest of this section we present a quick review of this work.

2.1. Differentiable Contour Case

Let $C \in \mathbb{R}^2$ be a twice-differentiable contour of length L and let $E_{2D,R}$ be the energy of an uniform charge distributed along C defined by

$$E_{2D,R}(C) = \frac{1}{2} \int \int_{C \times C} \left(\frac{1}{\|\mathbf{C}(s) - \mathbf{C}(\hat{s})\|} - \frac{1}{d_C(s,\hat{s})} \right) d\hat{s}\, ds, \quad (1)$$

where $d_C(s,\hat{s})$, the geodesic distance along the curve C from point $\mathbf{C}(s)$ to point $\mathbf{C}(\hat{s})$, is used to eliminate the infinite component of the first term, thereby making the energy finite. However the gradient of this energy has the property of still becoming infinitely large whenever the curve becomes close to self-intersection.

Using the Calculus of Variations, it is shown in [5] that the gradient of (1) is given by

$$\mathbf{R}_{2D}(s) = \lim_{\varepsilon \to 0^+} \left[\int_{B_C(\varepsilon,s)} \frac{\mathbf{C}(s) - \mathbf{C}(\hat{s})}{\|\mathbf{C}(s) - \mathbf{C}(\hat{s})\|^3} \cdot \mathbf{N}(s)\, d\hat{s} \right.$$
$$\left. + \int_{B_C(\varepsilon,s)} \frac{d\hat{s}}{\|\mathbf{C}(s) - \mathbf{C}(\hat{s})\|} \kappa(s) - \ln\left(\frac{L}{2\varepsilon} \right) \kappa(s) \right] \mathbf{N}(s), \quad (2)$$

where $B_C(\varepsilon,s) = \left\{ \mathbf{C}(\hat{s}) : d_C(\hat{s},s) > \varepsilon \right\}$ represents the set of all points in C except for those within a small neighborhood of $\mathbf{C}(s)$, and $\kappa(s)$ and $\mathbf{N}(s)$ represent the curvature and the inward normal of C at the point $\mathbf{C}(s)$, respectively. The first term in (2) can be regarded as the

projection of the electric vector field of the charge distribution at the point $\mathbf{C}(s)$ onto the inward normal $\mathbf{N}$. On the other hand, the second term can be regarded as the electrostatic potential of the charge distribution at the point $\mathbf{C}(s)$.

Now, let us suppose that C is evolved according to the image based flow $\mathbf{C}_{t,original}(s)$ that is uniformly bounded. Sundaramoorthi and Yezzi [5] show that if the flow $\mathbf{R}_{2D}(s)$ in (2) is added to $\mathbf{C}_{t,original}(s)$, then the topology of C will be preserved during the evolution. That is, the resulting flow

$$\mathbf{C}_{t,new}(s) = \mathbf{C}_{t,original}(s) + \mu_R \mathbf{R}_{2D}(s), \quad (3)$$

where t is the artificial time variable and μ_R is a positive constant, preserves the topology of C. Moreover, since (3) is a geometric flow, this method of topology preservation is suitable for both parametric particle-based and level set implementations.

2.2. Polygon Case

Let P be a polygon with N edges C_i for $i \in \{1,\dots,N\}$, each one of length $|C_i|$ and going from vertex $\mathbf{v}_i$ to vertex $\mathbf{v}_{i+1}$, both in $\mathbb{R}^2$. In addition, consider the electrostatic energy

$$E_{2D,R}(P) = 2\sum_i \left(|C_i| \ln |C_i| - |C_i| \right)$$
$$+ \frac{1}{2} \sum_{i \neq j} \iint_{C_i \times C_j} \frac{d\hat{s}\, ds}{\left\| \mathbf{C}_i(s) - \mathbf{C}_j(\hat{s}) \right\|}, \quad (4)$$

where the first term results from taking just the finite part of the integral $\iint_{C_i \times C_i} \frac{d\hat{s}\, ds}{\left\| \mathbf{C}(s) - \mathbf{C}(s) \right\|}$ and discarding the infinite component. Like the energy for the differentiable contour case (1), this energy only becomes infinitely large when the polygon approaches a topology change.

Let $\mathbf{R}_{2D,k}(t)$ be the gradient descend flow of (4) for vertex $\mathbf{v}_k$ at time t that is computed by the procedure outlined in [5] and let $\left(d\mathbf{v}_k / dt \right)_{original}$ be the original image based vertex flow. Sundaramoorthi and Yezzi [5] show that the new vertex flow

$$\left(\frac{d\mathbf{v}_k}{dt} \right)_{new} = \left(\frac{d\mathbf{v}_k}{dt} \right)_{original} + \mu_R R_{2D,k}(t) \quad (5)$$

has the property of preserving the topology of P during the evolution.

3. Topology Preservation in 3D

In many applications, such as 3D segmentation, a surface is evolved in order to solve a specific problem. Sometimes these applications require that the topology of the surface be preserved during the evolution. In such

cases it is necessary to use a topology preservation method. We now present the extension of the work in [5] to both active surfaces and active polyhedrons, making more emphasis on the latter since we will apply this in the next section.

3.1. Differentiable Surface Case

Let $S : [0,1] \times [0,1] \rightarrow \mathbb{R}^3$ be a parameterization of a differentiable, closed, compact and orientable surface, then the natural 3D extension of (1) is

$$E_{3D,R}(S) = \iint_{S \times S} \left[\frac{1}{\left\| \mathbf{S}(u,v) - \mathbf{S}(\hat{u},\hat{v}) \right\|^2} - \frac{1}{d_s^2((u,v),(\hat{u},\hat{v}))} \right] d\mathbf{S}\, d\mathbf{S}, \quad (6)$$

where $d_s((u,v),(\hat{u},\hat{v}))$ is the geodesic distance along the surface S from point $\mathbf{S}(u,v)$ to point $\mathbf{S}(\hat{u},\hat{v})$. However, unlike the case of curves, the second term is not straightforward to compute numerically nor is the variation easy to compute. Therefore, we consider the cut-off energy

$$E_{3D,R}(S) = \iint_{S \times B_\varepsilon} \frac{1}{\left\| \mathbf{S}(u,v) - \mathbf{S}(\hat{u},\hat{v}) \right\|^2} d\mathbf{S}\, d\mathbf{S}, \quad (7)$$

where $B_\varepsilon = \left\{ (\hat{u},\hat{v}) \in [0,1]^2 : |u - \hat{u}| \geq \varepsilon \vee |v - \hat{v}| \geq \varepsilon \right\}$ represents the set of all the points of S except for a small neighborhood around the point $\mathbf{S}(u,v)$.

A formal computation using the Calculus of Variations shows that the limit of the gradient of (7) converges and that it is equal to

$$\mathbf{R}_{3D}(u,v) = \lim_{\varepsilon \to 0^+} \left\{ \iint_{B_\varepsilon(S)} \left[\frac{\mathbf{S}(u,v) - \mathbf{S}(\hat{u},\hat{v})}{\left\| \mathbf{S}(u,v) - \mathbf{S}(\hat{u},\hat{v}) \right\|^4} \cdot \mathbf{N}(u,v) \right. \right.$$
$$\left. \left. + \frac{H(u,v)}{\left\| \mathbf{S}(u,v) - \mathbf{S}(\hat{u},\hat{v}) \right\|^2} \right] d\mathbf{S}(\hat{u},\hat{v}) \right\} \mathbf{N}(u,v), \quad (8)$$

where $H(u,v)$ and $\mathbf{N}(u,v)$ represent the mean curvature and the inward normal of S at $\mathbf{S}(u,v)$. We believe that $\mathbf{R}_{3D}$ becomes infinite as the surface approaches self-intersection and points in a direction opposite to self-intersection, as in the case of curves. Analytical details will be found in an upcoming paper. We offer experimental evidence in Section 5.

3.2. Triangulated Surface Case

Topology preservation methods can also be applied to active polyhedron, that is, a polyhedral surface whose vertices evolve to minimize some energy functional. In this sense, Slabaugh and Unal [4] have proposed a 3D extension of the work in [3] by adding an electric force to each vertex flow. This force is computed by creating an electric field that goes to infinity as a vertex moves

towards the surface. Unfortunately, this method does not guarantee topology preservation between non-adjacent triangular faces and becomes unstable as the triangular mesh becomes finer. This is especially true for our novel cortical unfolding application that we present in the next section, which needs topology preservation to work properly. Therefore, we decided to choose a direct energy-based approach based on [5], which although slower, provides a more powerful topology preservation factor.

Let S be a triangulated surface with N faces S_i for $i \in \{1, \ldots, N\}$. Let also $\mathbf{v}_a$, $\mathbf{v}_b$, and $\mathbf{v}_c$ be the vertices of S_i, ordered counterclockwise, as shown in Fig. 1. Now consider the new energy

$$E_{3D,R} = \sum_{i=1}^{N} \sum_{j=1, j \neq i}^{N} E_{3D,R_{i,j}}, \qquad (9)$$

where $E_{3D,R_{i,j}}$ represents the electrostatic energy between the faces S_i and S_j. More specifically, $E_{3D,R_{i,j}}$ is defined by

$$E_{3D,R_{i,j}} = \iint_{S_i \times S_j} \frac{1}{\left\| \mathbf{S}_i - \mathbf{S}_j \right\|^2} dS_i \, dS_j. \qquad (10)$$

Accordingly, the gradient proposed energy in (9) becomes infinitely large when any two faces become infinitely close.

Taking the derivative of $E_{3D,R}$ with respect to the vertex $\mathbf{v}_a$ of S_i gives us

$$\frac{\partial E_{3D,R}}{\partial \mathbf{v}_a} = \sum_{i=1}^{N} \sum_{j=1, j \neq i}^{N} \frac{\partial E_{3D,R_{i,j}}}{\partial \mathbf{v}_a}. \qquad (11)$$

Furthermore, if we use the parameterization

$$\mathbf{S}_i(u,v) = \mathbf{v}_a + u(\mathbf{v}_b - \mathbf{v}_a) + v(\mathbf{v}_c - \mathbf{v}_a), \qquad (12)$$

for $u \in [0,1]$ and $v \in [0, 1-u]$, then it can be shown that the derivative of $E_{3D,R_{i,j}}$ with respect to $\mathbf{v}_a$ in (11) when S_i and S_j are non-adjacent becomes

$$\frac{\partial E_{3D,R_{i,j}}}{\partial \mathbf{v}_a} = -8 A_i A_j \int_0^1 \int_0^{1-u} \int_0^1 \int_0^{1-\hat{u}} (1 - u - v) \mathbf{F}_{i,j} \, d\hat{v} \, d\hat{u} \, dv \, du$$
$$+ 4 A_j \int_0^1 \int_0^{1-u} \int_0^1 \int_0^{1-\hat{u}} \frac{1}{\left\| \mathbf{S}_i(u,v) - \mathbf{S}_j(\hat{u},\hat{v}) \right\|^2} d\hat{v} \, d\hat{u} \, dv \, du \, \frac{\partial A_i}{\partial \mathbf{v}_a}, \qquad (13)$$

where

$$A_i = \frac{1}{2} \left\| (\mathbf{v}_b - \mathbf{v}_a) \times (\mathbf{v}_c - \mathbf{v}_a) \right\| \qquad (14)$$

is the area of S_i and the force vector $\mathbf{F}_{i,j}$ is given by

$$\mathbf{F}_{i,j} = \frac{\mathbf{S}_i(u,v) - \mathbf{S}_j(\hat{u},\hat{v})}{\left\| \mathbf{S}_i(u,v) - \mathbf{S}_j(\hat{u},\hat{v}) \right\|^4}. \qquad (15)$$

If S_i and S_j are adjacent, then the derivative of $E_{3D,R_{i,j}}$ with respect to $\mathbf{v}_a$ is different from (13). Without loss of generality, let us assume that S_i and S_j share at least the vertex $\mathbf{v}_a$ in Fig. 1. It can be verified that
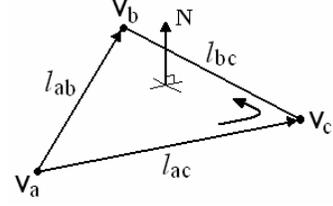
Figure 1: Sample triangle S_i for a triangular mesh.

$$\frac{\partial E_{3D,R_{i,j}}}{\partial \mathbf{v}_a} = -8 A_i A_j \int_0^1 \int_0^{1-u} \int_0^1 \int_0^{1-\hat{u}} (\hat{u} + \hat{v} - u - v) \mathbf{F}_{i,j} \, d\hat{v} \, d\hat{u} \, dv \, du$$
$$+ 4 A_j \int_0^1 \int_0^{1-u} \int_0^1 \int_0^{1-\hat{u}} \frac{1}{\left\| \mathbf{S}_i(u,v) - \mathbf{S}_j(\hat{u},\hat{v}) \right\|^2} d\hat{v} \, d\hat{u} \, dv \, du \, \frac{\partial A_i}{\partial \mathbf{v}_a} \qquad (16)$$
$$+ 4 A_i \int_0^1 \int_0^{1-u} \int_0^1 \int_0^{1-\hat{u}} \frac{1}{\left\| \mathbf{S}_i(u,v) - \mathbf{S}_j(\hat{u},\hat{v}) \right\|^2} d\hat{v} \, d\hat{u} \, dv \, du \, \frac{\partial A_j}{\partial \mathbf{v}_a},$$

for $\mathbf{F}_{i,j}$ defined as in (15).

Although the computation of (13) implies the numerical solution of quadruple integrals, we can reduce the number of computations by solving it explicitly just when the two faces S_i and S_j are close enough, that is, when they are within a certain thresholded distance from each other, which is when it matters the most. On the other hand, when the faces are not considered to be close enough we can then use their centroids, which we called $\bar{\mathbf{S}}_i$ and $\bar{\mathbf{S}}_j$, in (10). The result is the much simpler estimate

$$\frac{\partial E_{3D,R_{i,j}}}{\partial \mathbf{v}_a} = -\frac{2}{3} A_i A_j \frac{\bar{\mathbf{S}}_i - \bar{\mathbf{S}}_j}{\left\| \bar{\mathbf{S}}_i - \bar{\mathbf{S}}_j \right\|^4} + \frac{A_j}{\left\| \bar{\mathbf{S}}_i - \bar{\mathbf{S}}_j \right\|^2} \frac{\partial A_i}{\partial \mathbf{v}_a}. \qquad (17)$$

Again, if we add the vertex motion as defined in (11), to a surface based evolution then the topology of the surface will be preserved during the evolution.

4. Application to Cortical Unfolding

In this section we present a novel viewpoint-based visibility energy as the basis for a class of flows with appropriate geometric constraints that can be used to maximize the visibility of a surface with respect to a fixed external viewpoint. Accordingly, a surface would evolve in such a way that would allow one to see parts that are not visible due to self-occlusion. This result can have several applications in the area of medical imaging. For instance, it can be used in human brain mapping to unfold a specific part of the cerebral cortex while introducing little distortion and to validate a cortex segmentation.

The proposed energy, although novel, cannot work by itself, as it requires topology preservation. For

completeness, we quickly present this energy and its gradient descent. More details about this energy are the subject of a different paper [15].

4.1. New Visibility Energy Functional for Viewpoint-Based Unfolding

Let S be a differentiable surface and let S_v be a selected region of interest on S that the user would like to unfold for visualization. The problem of maximizing the visibility of this portion S_v of the surface with respect to a fixed viewpoint $\mathbf{P}$ can be thought as the problem of maximizing the flux of light irradiated from $\mathbf{P}$ that is being absorbed by S_v. We define the flux at any point in S_v as the Euclidean dot product between the unit ray that is coming from $\mathbf{P}$ and the unit inward normal $\mathbf{N}$ of S_v at the given point. Accordingly, the value of the flux at any point will always be between -1 and 1. This approach provides a physical interpretation of how illuminated any point in S_v is. If a point is illuminated, that is, if it is visible from $\mathbf{P}$, a positive flux indicates the degree of perpendicularity of the incoming ray. On the other hand, if a point is not receiving any light because S_v is blocking the ray, a positive flux indicates how perpendicular the ray is going to come in if the part of S_v that is blocking the ray moves away. When a point has a negative flux then it means that the point is not receiving any light. The more negative the flux is, the more the point will have to move to receive light.

Consider the energy

$$E_{3D}(S_v) = \frac{1}{A_{S_v}} \iint_{S_v} \frac{\mathbf{S} - \mathbf{P}}{\|\mathbf{S} - \mathbf{P}\|} \cdot \mathbf{N}\, dS, \qquad (18)$$

where A_{S_v} is the area of S_v, $\mathbf{S} \in \mathbb{R}^3$ is a point in the surface, and $\mathbf{N} \in \mathbb{R}^3$ is the unit inward normal at $\mathbf{S}$. This energy represents the average visibility S_v with respect to $\mathbf{P}$. From now on, we will use the terms "average flux" and "average visibility" interchangeably.

If we evolve S_v according to the gradient ascent along (18), then the points where the flux is negative would be forced to move in such a way that the flux they receive increases. By doing so, these points would make visible other points that already have a positive flux, but are not visible from $\mathbf{P}$. This would generate the unfolding motion that we are looking for.

Since the flux at any point can be at most equal to 1, then $E_{3D}(S_v)$ also has a maximum of 1. This would occur when the viewing surface coincides with a circular arc with the viewpoint $\mathbf{P}$ as its center. In this case, the rays coming from the viewpoint would have the same direction as the unit inward normal at each point and, consequently, the flux at every point in S_v would be equal to 1.

Using the Calculus of Variations, it can be shown that a maximizing gradient flow for (18) is given by

$$\mathbf{S}_t = \frac{1}{A_{S_v}}\left(H\, E_{3D}(S_v) + \frac{1}{\|\mathbf{S} - \mathbf{P}\|}\right)\mathbf{N}, \qquad (19)$$

where H represents the mean curvature of S_v at the point $\mathbf{S}$. This result gives us the main formulation in case we want to implement the proposed method for differentiable contours. In addition, it provides us with a mathematical criterion that tells us which part of the surface we can flatten. Specifically, this stability condition is that we must choose the portion S_v of the surface to have a positive initial average visibility (otherwise a backwards heat flow results). This may be done by enlarging or reducing the initial region S_v until this condition is satisfied. As the surface unfolds, the average visibility of S_v increases thereby allowing a user to select a smaller subset of S_v at later stages.

4.2. Triangulated Surface Case

Let S be now a triangulated mesh and let S_v be a section of S with N triangles and a positive average visibility with respect to the viewpoint $\mathbf{P}$. By applying (18) to S_v we get that the average visibility of S_v, $E_{3D,P}$, is

$$E_{3D,P}(S) = \frac{1}{A_{S_v}} \sum_{i=1}^{N} E_{3D,i}, \qquad (20)$$

where $A_{S_v} = A_{S_1} + \ldots + A_{S_N}$ is the total area of S_v and $E_{3D,i}$ represents the total flux being received by the triangular face S_i of area A_i. Accordingly, $E_{3D,i}$ is

$$E_{3D,i} = \iint_{S_i} \frac{\mathbf{S}_i - \mathbf{P}}{\|\mathbf{S}_i - \mathbf{P}\|} \cdot \mathbf{N}\, dS_i, \qquad (21)$$

where the inward normal $\mathbf{N}$ (Fig. 1) is given by

$$\mathbf{N} = -\frac{(\mathbf{v}_b - \mathbf{v}_a) \times (\mathbf{v}_c - \mathbf{v}_a)}{\|(\mathbf{v}_b - \mathbf{v}_a) \times (\mathbf{v}_c - \mathbf{v}_a)\|}. \qquad (22)$$

If we use the parameterization in (12) it can be show that (21) becomes

$$E_{3D,i} = \frac{\alpha}{l_{ac}} \int_0^1 \ln\left(\frac{l_{ac}^2(1-u) + \beta + \gamma\, l_{ac}}{\beta + \delta\, l_{ac}}\right) du, \qquad (23)$$

for

$$\alpha = -(\mathbf{v}_a - \mathbf{P}) \cdot (\mathbf{v}_a \times \mathbf{v}_b + \mathbf{v}_b \times \mathbf{v}_c + \mathbf{v}_c \times \mathbf{v}_a), \qquad (24)$$

$$\beta = (\mathbf{v}_c - \mathbf{v}_a) \cdot ((1-u)\mathbf{v}_a + u\mathbf{v}_b - \mathbf{P}), \qquad (25)$$

$$\gamma = \|u\mathbf{v}_b + (1-u)\mathbf{v}_c - \mathbf{P}\|, \qquad (26)$$

and

$$\delta = \|(1-u)\mathbf{v}_a + u\mathbf{v}_b - \mathbf{P}\|. \qquad (27)$$

Taking the derivative of $E_{3D,i}$ with respect to the vertex $\mathbf{v}_a$ we get

$$\frac{\partial E_{3D,i}}{\partial \mathbf{v}_a} = \frac{\alpha}{l_{ac}} \int_0^1 \left[\frac{\left(2(1-u)+\gamma/l_{ac}\right)\left(\mathbf{v}_a - \mathbf{v}_c\right) + \partial\beta/\partial\mathbf{v}_a}{l_{ac}^2(1-u)+\beta+\gamma\, l_{ac}} \right.$$

$$\left. - \frac{\partial\beta/\partial\mathbf{v}_a + l_{ac}\,\partial\delta/\partial\mathbf{v}_a + \delta/l_{ac}\left(\mathbf{v}_a - \mathbf{v}_c\right)}{\beta+\delta\, l_{ac}} \right]du \quad (28)$$

$$+ E_{3D,i}/\alpha\left(\partial\alpha/\partial\mathbf{v}_a - \alpha/l_{ac}^2\left(\mathbf{v}_a - \mathbf{v}_c\right)\right),$$

where the partial derivatives of α, β, and δ with respect to $\mathbf{v}_a$ can be obtained from (24), (25), and (27), respectively. On the other hand, if we take the derivative of (20) with respect to $\mathbf{v}_a$ we get

$$\frac{\partial E_{3D,P}(S)}{\partial \mathbf{v}_a} = \frac{1}{A_{S_v}} \sum_{i=0}^{N-1} \left(\frac{\partial E_{3D,i}}{\partial \mathbf{v}_a} - E_{3D,P}(S)\frac{\partial A_i}{\partial \mathbf{v}_a} \right). \quad (29)$$

Using these results together with those of the previous section we have that the vertex motion that maximizes the average visibility of S_v (20), while preserving its topology, is given by

$$\frac{d\mathbf{v}_a}{dt} = \mu_{3D} \frac{\partial E_{3D,P}}{\partial \mathbf{v}_a} + \mu_R \frac{\partial E_{3D,R}}{\partial \mathbf{v}_a}, \quad (30)$$

where μ_{3D} and μ_R are positive constants and the second term is the topology preserving term computed by using (11).

4.3. Area Preservation

In order to have an average visibility equal to 1, the region of interest S_v in the triangulated mesh S has to have a visibility equal to 1 at every point of every one of its faces. It is easy to see that this only occurs when all the faces collapse to a single point. Of course, this result is undesirable. To overcome this issue we need to maximize the average visibility and, at the same time, maintain the area of each one of the triangular faces of S_v constant. This can be done by applying a similar technique such as the one employed in [16, 17, 18] in which only the component of the gradient that does not change the area is used to evolve the vertices. This procedure is described below.

Let $\Psi = \{\mathbf{v}_1,\ldots,\mathbf{v}_M\}$ be the ordered set of the M 3D vertices comprising S_v. In order to maintain a constant area for each of the triangular faces S_i in S_v during the evolution we need to satisfy the following N constraints

$$\frac{1}{2}\left\|\left(\mathbf{v}_{i,b} - \mathbf{v}_{i,a}\right)\times\left(\mathbf{v}_{i,c} - \mathbf{v}_{i,a}\right)\right\|^2 - A_i^2 = 0, \quad (31)$$

where $i \in \{1,\ldots,N\}$ and the vectors $\mathbf{v}_{i,a}$, $\mathbf{v}_{i,b}$, and $\mathbf{v}_{i,c}$ represent the corresponding vertices of S_i (see Fig. 1) in Ψ. Using Lagrange multipliers one can obtain

$$V_{t,c} = V_{t,u} - J^T\mathbf{l}, \quad (32)$$

where $V_{t,u}$ is the vector of unconstrained gradient flow
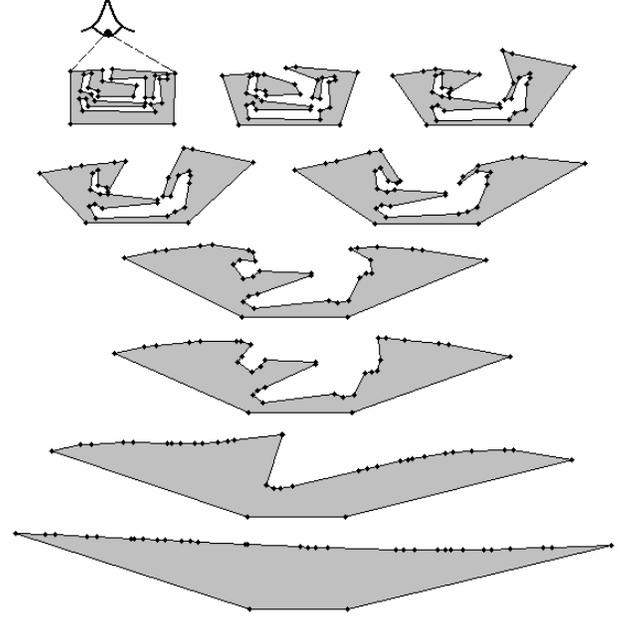
Figure 2: Visibility maximization evolution for a highly convoluted polygon.
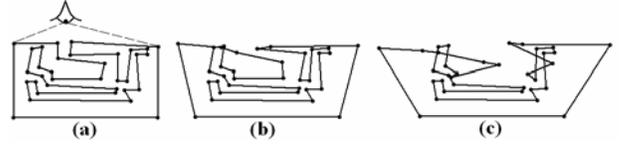
Figure 3: Visibility maximization without topology preservation. (a) Initial polygon. (b) Polygon after 10 iterations. (c) Polygon after 100 iterations.

obtained by applying (30) to each vertex of S_v, J is the Jacobian matrix of (31), $V_{t,c} = \frac{d}{dt}\left[\mathbf{v}_1^T...\mathbf{v}_M^T\right]^T$ is the vector of constrained gradient flow, and the vector $\mathbf{l}$ is the minimum norm solution to the system

$$JJ^T\mathbf{l} = JV_{t,u}. \quad (33)$$

Since the matrix JJ^T is symmetric positive definite, then $\mathbf{l}$ can be quickly computed using the conjugate gradient method. Moreover, since J is sparse, the matrix multiplication JJ^T can be computed and stored efficiently.

5. Simulation Results

In order to better illustrate how the proposed topology preservation method works together with the proposed visibility energy functional of Section 4, we first present a 2D example. Figure 2 depicts the evolution of a very convoluted 34-edge polygon in which the region of interest is the section of the contour located between the two lines of sight. Initially the region of interest had an
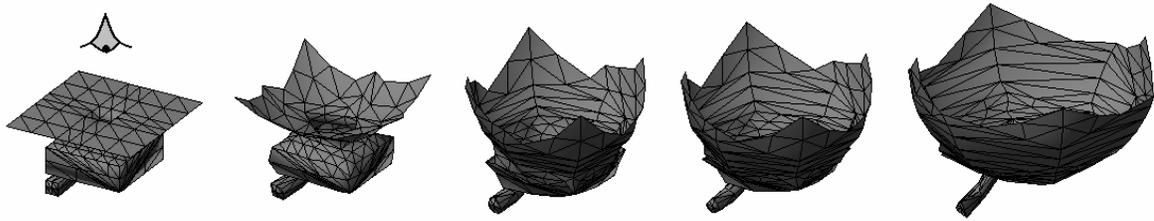
Figure 4: Unfolding of a synthetic triangulated surface using the proposed visibility maximization approach.
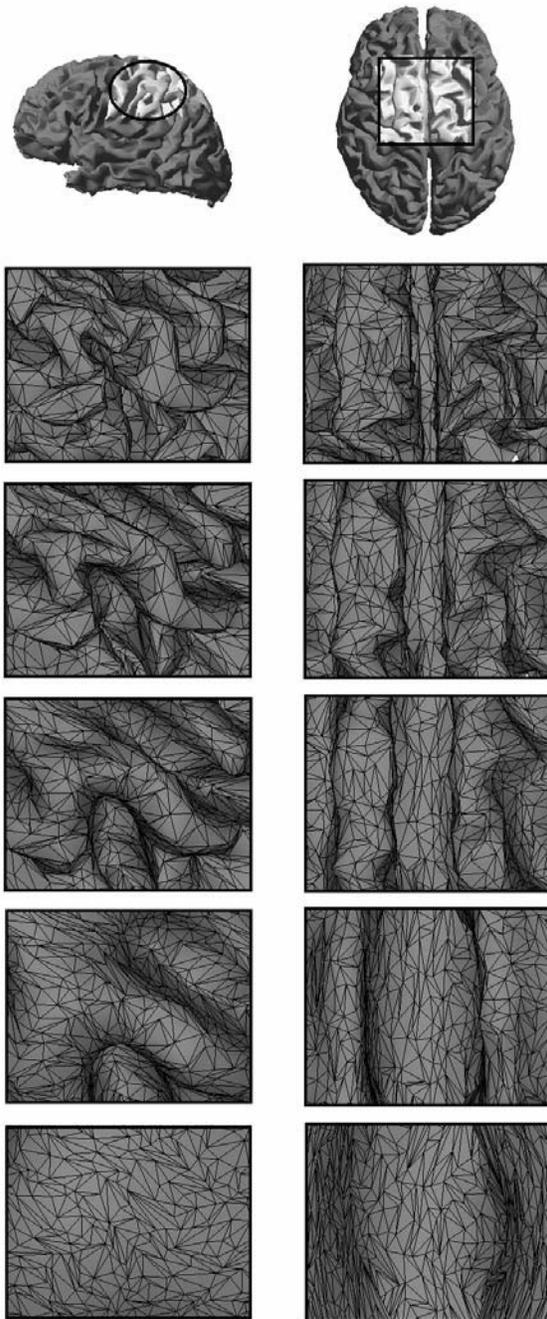
Figure 5: Unfolding of for two different regions of a cortex using visibility maximization.

average visibility of just 0.17. As the 2D version of the visibility maximization algorithm is applied, the polygon unfolded to make visible sections that were previously not visible. Indeed, by the end of the simulation the average visibility of the region of interest was almost equal to 1.

Figure 3 shows the importance of having topology preservation. In this simulation we applied the proposed algorithm without the topology preserving forces to the highly convoluted polygon of Fig. 2. As can be seen, the edges started to intersect each other after a few iterations.

Figure 4 depicts the evolution of a 3D synthetic surface when the visibility is maximized and, at the same time, the topology is preserved. The initial visibility of this surface was 0.2, whereas by the end of the simulation it was very close to 1.

Topology preservation plays a very important role when the surface for which the visibility is going to be maximized is very convoluted. This is the case of the evolutions shown in Fig. 5, where two regions of a cortex are evolved so that the visibility with respect to a viewpoint located just in front of the regions is maximized. Figure 6 shows an additional evolution in which one can clearly see how the selected region unfolds to become more visible from the external viewpoint.

6. Conclusion

We have presented a novel method for cortical surface unfolding based on a viewpoint based visibility energy and a three dimensional generalization of knot energy type forces for topology preservation. Simulation results show that the gradient flow of these combined energy terms yields a useful localized unfolding of the cortical surface specially tailored to the user's current viewpoint. We believe this method, compared with more traditional global flattening techniques, may be very useful for more customized inspection of cortical surface segmentations. Methods to reduce the computational cost will be the primary focus of future research in order to make the approach more user interactive in real time.

References

[1] Han, C. Xu, D. Tosun, and J. L. Prince. Cortical surface reconstruction using a topology preserving geometric

deformable model. Proceedings of MMBIA, 213-220, 2001.

[2] X. Han, C. Xu, and J. L. Prince. A topology preserving level set method for geometric deformable models. IEEE Trans. on Pattern Analysis and Machine Intelligence, 25(6):755-768, 2003.

[3] G. Unal, A. Yezzi, and H. Krim. Information-theoretic active polygons for unsupervised texture segmentation. International Journal of Computer Vision, 62(3):199-220, 2005.

[4] G. Slabaugh and G. Unal. Active polyhedron: surface evolution theory applied to deformable meshes. Proceedings of CVPR, 84-91, 2005.

[5] G. Sundaramoorthi and A. Yezzi. More-than-topology-preserving flows for active contours and polygons. Proceedings of ICCV, 1276-1283, 2005.

[6] J. O'Hara. Energy of a knot. Topology, 30:241-247, 1991.

[7] A. Abrams, J. Cantarella, J. Fu, M. Ghomi, and R. Howard. Circles minimize most knot energies. Topology, 42:381-394, 2003.

[8] Y. Shi and W. C. Karl. Differentiable minimin shape distance for incorporating topological priors in biomedical imaging. IEEE International Symposium on Biomedical Imaging, 1247-1250, 2004.

[9] O. Alexandrov and F. Santosa. A topology-preserving level set method for shape optimization. Journal of Computational Physics, 204:121-130, 2005.

[10] C. Le Guyader and L. Vese. Self-repelling snakes for topology segmentation models. Technical Report, UCLA, 2007.

[11] S. Osher and J. Sethian. Fronts propagating with curvature-dependent speed: algorithms based on the Hamilton-Jacobi equations. Journal of Computational Physics, 79:12-49, 1988.

[12] S. Angenet, S. Haker, A. Tannenbaum, and R. Kikinis, On the Laplace-Bertrami operator and brain surface flattening. IEEE Transactions on Medical Imaging, 18(80):700-711, 1999.

[13] G. Hermosillo, O. Faugeras, and J. Gomes. Cortex unfolding using level set methods. Technical Report 3663, INRIA, 1999.

[14] J-P. Pons, R. Keriven, and O. Faugeras. Area preserving cortex unfolding. MICCAI, 376-383, 2004.

[15] K. Rocha, A. Yezzi, A. Mennucci, and J. L. Prince. Viewpoint-based visibility maximizing flows. To be presented at the 2007 MICCAI Workshop on Interaction in medical image analysis and visualization.

[16] A. Witkin and D. Baraff. Physically Based Modeling: Principles and Practice. SIGGRAPH'97 Course Notes, 1-13, 1997.

[17] J. H. Cantarella, E. D. Demaine, H. N. Iben, and J. F. O'Brian. An energy-driven approach to linkage unfolding. Proceedings of the 20th Symposium on Computational Geometry, 134-143, 2004.

[18] H. N. Iben, J. R. O'Brien, and E. D. Demaine. Refolding planar polygons. Proceedings of the 22nd Symposium. on Computational Geometry, 71-79, 2006.
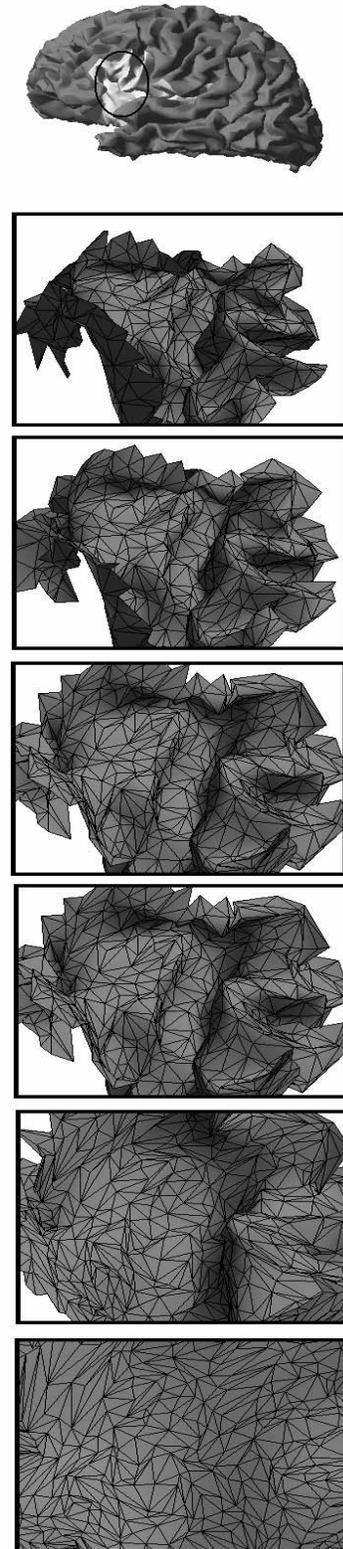
Figure 6: Unfolding of a region of the cortex using viewpoint-based visibility maximization.